ELSEVIER

Ceramics International 32 (2006) 147–156

CERAMICS INTERNATIONAL

www.elsevier.com/locate/ceramint

Dispersion of lanthanoid-coated barium titanate in a paraffin-based extrusion binder system

Markus Wegmann [a,b,*], Frank Clemens [a], Alan Hendry [b], Thomas Graule [a]

[a] *Laboratory for High Performance Ceramics, Swiss Federal Laboratories for Materials Testing and Research (EMPA), CH-8600 Dübendorf, Switzerland*

[b] *Materials and Metallurgy Group, Department of Mechanical Engineering, University of Strathclyde, Glasgow G1 XXJ, UK*

Received 17 December 2004; received in revised form 13 January 2005; accepted 13 January 2005
Available online 3 May 2005

This work is dedicated to the memory of Professor Alan Hendry.

Abstract

For the fabrication of small $BaTiO_3$-based PTCR elements by ceramic powder extrusion, a submicron barium titanate ($BaTiO_3$) powder was coated with either CeO_2 or La_2O_3 and mixed with a paraffin-based thermoplastic binder. XPS analysis revealed that the powder surfaces are significantly hydrated and that processing aids are likely to interact with the physisorbed and chemisorbed water rather than directly with the ceramic powder surfaces. From a series of potential C-18 surfactants for this paraffin-based extrusion system, stearic acid was shown to be the most effective dispersant and was consequently used to prepare extrusion feedstocks. Under equivalent extrusion conditions, 50 vol.% CeO_2-coated $BaTiO_3$ feedstocks always exhibited poorer extrudability than their La_2O_3-coated $BaTiO_3$ counterparts. Furthermore, the La-doped material invariably sintered to a higher final density than the Ce-doped material. These processability differences can largely be explained by a lower affinity of the stearic acid surfactant for the CeO_2-coated titanate powder.

Keywords: A. Extrusion; A. Mixing; B. Fibres; D. $BaTiO_3$ and titanates; E. PTC devices

1. Introduction

Barium titanate ($BaTiO_3$) is a technologically important ceramic in the area of electronics, being used extensively in the manufacture of capacitors, piezoelectric transducers and actuators, and positive temperature coefficient of resistivity (PTCR) elements. Further, it is of growing interest for use in dynamic random access memories and optoelectronics. The majority of components for these applications are formed by consolidating powders into the desired bulk geometries by a variety of shaping methods, including pressing, tape casting, extrusion and injection moulding. As is generally the case in ceramic powder processing, successful consolidation of $BaTiO_3$ powders into homogeneous bodies of high green density requires the powders to be deagglomerated and dispersed in a suitable fluid medium (solvent and/or binder) during the forming process, and this in turn requires the use of surfactants/dispersants to form a chemical bridge between the ceramic powder surface and the fluid binder phase. Binder systems for $BaTiO_3$ processing may be either aqueous-based (e.g. for slip casting [1], extrusion [2], tape casting [3–5]) or organic solvent-based (e.g. for pressure filtration [6], tape casting [3,7,8]). Here, the former are complicated by the effect of $BaCO_3$ dissolution on the electrostatic stabilisation of the powder particles [1,5,9,10], and the latter by health and environmental concerns over the use of organic solvents.

These and other issues had to be considered by the authors of the current work while developing the extrusion process for the fabrication of lanthanoid-doped $BaTiO_3$ filaments for PTCR applications [11]. PTCR thermistors based on barium titanate ($BaTiO_3$ doped with, e.g. Y, Sc, La, the range 0.1–0.6 mol%) exhibit unique resistance versus temperature behaviour which is characterized by relatively

* Corresponding author.

0272-8842/$30.00
doi:10.1016/j.ceramint.2005.01.011

low electrical resistivity (10–100 Ω cm) when the material is in its low-temperature tetragonal ferroelectric state, and a resistance 3–7 orders of magnitude higher when it is heated into its high-temperature cubic paraelectric state [12] either by internal (I^2R) heating, or by an external heat source. For pure $BaTiO_3$, this transition temperature (T_c) between the two states is 130 °C. When the body temperature of the thermistor is returned to a level below T_c, the material returns to its low-resistance state. Because the switching process, which can be repeated many thousands of times by the same piece of ceramic, depends on heating a mass of material, the physical size of a thermistor is instrumental in determining the rate of its response to internal and external heating. Reducing the thermal mass of the thermistor reduces its response time and hence dramatically improves its ability to react to rapid transients in heat or power. The authors have fabricated very small, free-standing PTCR thermistors with such rapid-response capability by extrusion (fibres 0.25 and 0.125 mm diameter, 2 mm long), and the small minimum dimensions of the filaments demanded particular care to be taken when dispersing $BaTiO_3$ powder in the binder phase needed to enable forming: The small die diameters to be used in the microextrusion process (≤300 μm) dictated that the feed-powder have a primary particle size distribution in the submicron range, and that the powder be dispersed in the binder in a totally deagglomerated state. Furthermore, the binder phase/powder combination ideally needed to be pseudoplastic with a yield point in order for the system to flow easily during extrusion and for the extrudate to maintain its shape after the forming process. Finally, the binder was not to phase-separate from the powder under pressure and shear during extrusion.

The work performed by the authors to develop the binder system for the extrusion process is described in the current paper. A simple paraffin wax-based thermoplastic binder system of the type used for low-pressure injection moulding of SiC [13,14], Al_2O_3 [15,16] and ZrO_2 [17] was chosen to enable processing of extrudable feedstocks. The use of a thermoplastic binder permitted the problems encountered with aqueous and organic solvents mentioned above to be largely avoided, and the inherent low viscosity of the low-molecular-weight paraffin wax promised to yield low-viscosity feedstocks which would minimise abrasive wear of the processing equipment (mixer, extruder) and therefore undesired contamination of the $BaTiO_3$ ceramic composition. This latter point was very important as ppm concentrations of metallic elements (e.g. Fe, Mn) can have a significant effect on the PTCR behaviour of lanthanoid-doped $BaTiO_3$ materials [12].

The nominal PTCR compositions used throughout the work were $Ba_{0.9975}Ce_{0.0025}TiO_3$ and $Ba_{0.9985}La_{0.0015}TiO_3$. Lanthanoid-doped barium titanate exhibits appreciable electronic conductivity at room temperature in only a very narrow dopant concentration range, and the cerium and lanthanum concentrations used here coincide with the maxima in the plots of room-temperature conductivity versus dopant level for the two systems sintered in air. Because doped submicrometre $BaTiO_3$ powders suitable for the extrusion of filaments with diameters below 300 μm were not commercially available, a fine $BaTiO_3$ powder had to first be doped accordingly.

The specific aim of the work reported here was to select a suitable surfactant from a series of 18-carbon (C-18) dispersant molecules and then to produce extrudable feedstocks of the lanthanoid-coated powders.

2. Experimental procedure

2.1. Coated powder preparation

$BaTiO_3$ powder (Ticon F, Ferro Electronic Materials, Niagara Falls NY, USA; $d_{50} = 0.5$ μm, $d_{90} = 0.8$ μm; SSA ≈ 6.6 m^2/g) was coated with the dopants by dispersing the powder in an aqueous solution of the corresponding nitrate ($Ce(NO_3)_3{\cdot}6H_2O$ or $La(NO_3)_3{\cdot}6H_2O$; >99.9%, Sigma–Aldrich), evaporating off the water, calcining under static air to yield the dopant oxide, and grinding the resulting powder. A sintering aid $4Al_2O_3$–$9SiO_2$–$3TiO_2$ (AST [18]; 1 mol% based on $BaTiO_3$) was subsequently added to the coated powders by dispersing them in an aqueous suspension of nanometre-sized powders of Al_2O_3 (“high purity”, BDH/Merck), SiO_2 (99.8%, Sigma–Aldrich) and TiO_2 (99.9%, Alfa Aesar) and drying and grinding again. These procedures resulted in only slight coarsening/agglomeration of the powders (CeO_2-coated: $d_{50} = 0.6$ μm, $d_{90} = 2.3$ μm; La_2O_3-coated: $d_{50} = 0.5$ μm, $d_{90} = 2.0$ μm) [11].

The powder surfaces were characterised at room temperature (RT) and 400 °C using X-ray photoelectron spectroscopy (XPS; ESCA 3 Mk.II, VG Scientific Ltd., East Grinstead, West Sussex, UK). Samples were measured and data analysed as described in detail elsewhere [19]. Measurements were performed with Mg Kα radiation (1253.6 eV) at ≈10^{-8} Pa and binding energies (BE) referenced to the C 1s line of graphite at 284.5 eV. For quantitative analysis of spectra, the peak backgrounds were removed by the linear tangent method [20].

2.2. Surfactant screening

Sedimentation experiments with suspensions of powder in molten paraffin wax (purum, $T_m = 50$–52 °C, Sigma–Aldrich) were performed to test the dispersing effectiveness of four C-18 organic surfactants (see Table 1): stearic acid (Ph Helv, Sigma–Aldrich), octadecylamine (tech., Sigma–Aldrich), oleic acid (tech., Sigma–Aldrich) and oleylamine (tech., Sigma–Aldrich). All possess a hydrophobic carbon chain (saturated or unsaturated) and a hydrophilic polar (carboxyl or amine) head group. These short-chained dispersants were chosen based on their proven ability to aid the dispersion of inorganic powders in organic media [21]. They have been shown to enable high powder loadings

Table 1
Surfactant species for $BaTiO_3$–paraffin mixtures

Name	Formula
Stearic acid	$CH_3(CH_2)_{16}COOH$
Octadecylamine	$CH_3(CH_2)_{17}NH_2$
Oleic acid	$CH_3(CH_2)_7CH{=}CH(CH_2)_7COOH$
Oleylamine	$CH_3(CH_2)_7CH{=}CH(CH_2)_8NH_2$

without generating excessively-thick adsorbed layers on the powder particles which can ultimately reduce the ceramic packing density [6].

Powder (10 vol.%) was dispersed in a given wax/surfactant mixture at 80 °C by simultaneous stirring and ultrasonic agitation. The processing temperature of 80 °C was chosen to be 10 °C above the highest melting temperature of the organic substances in use, i.e. that of stearic acid with $T_m = 70$ °C. The suspension was deaired under vacuum, poured into a preheated test tube, and then placed in an oven at 80 °C. Sediment height and elapsed time were recorded over a period of days. Two surfactant concentrations were tested, namely 1.2 wt.% w.r.t. paraffin (1.6 wt.% w.r.t. $BaTiO_3$) and 30 wt.% w.r.t. paraffin (28 wt.% w.r.t. $BaTiO_3$). The former approximates monolayer coverage based on the area occupied by an adsorbed stearic acid molecule (0.2 nm^2) [22] and the specific surface area of the powder, and the latter is a representative value (based on experience) for the concentration of surfactant in the binder phase in concentrated thermoplastic extrusion feedstocks.

2.3. Feedstock preparation and extrusion

The powder premixes were blended at 80 °C with paraffin wax binder and surfactant and subsequently extruded at 55 °C through circular cross-section dies (Ø = 60–300 μm), as described in detail elsewhere [11,23]. While solids loadings up to 60 vol.% were achieved, the current study was performed with solids loadings of 50 vol.%. Uncontrollable slip-stick behaviour of the more highly-loaded feedstocks prevented the rheological analyses described immediately below from being reliably performed.

The rheology of the feedstocks at 55 and 80 °C was analyzed in the shear-rate range 1–10 s^{-1} using rotational rheometry (CSL^{2}500 Carri-Med, TA Instruments, New Castle DE, USA) with a plate/plate geometry (1 cm diameter, 500 μm gap). Capillary rheometry (ACER Capillary Extrusion Rheometer, Rheometric Scientific, Piscataway NJ, USA) at the same temperatures was used to investigate flow behaviour in excess of 100 s^{-1}. Dies of 0.5 mm diameter with L/D ratios 10:1, 40:1, 100:1 and 200:1 were used and the Weissenberg–Rabinowitsch shear-rate and Bagley entry-pressure corrections were applied to the data [24].

Extrudates were debound under static air (1.5 °C/min to 400 °C, 5 °C/min to 700 °C, 1 h dwell). The pore-size distributions of presintered (1200 °C) samples were determined using mercury intrusion porosimetry (MIP; Model 140/440, CE Instruments Ltd., Wigan, UK).

2.4. General analyses

At the various stages of processing described above, samples were characterised using scanning electron microscopy (SEM), X-ray diffraction (XRD), thermal gravimetric analysis (TGA) and thermal mechanical analysis (TMA).

3. Results and discussion

3.1. Powder characteristics

The hydrophilic nature of $BaTiO_3$ is well documented [8,25–27], and the presence of physisorbed water was confirmed on the lanthanoid-coated powders by the XPS analysis. As shown in Fig. 1 for the CeO_2–$BaTiO_3$ case, the O 1s peak exhibits a high binding energy shoulder which is largely removed by heating to 400 °C and which reappears after exposure to atmosphere. This behaviour is identical to that observed in the XPS analysis of the as-received powder [19], and the conclusions for the current analysis are the same as previously: The main peak centred on 529.5 eV is attributed to oxygen in the $BaTiO_3$ lattice and the small high-BE shoulder which appears upon cooling in the sample chamber under vacuum is due to oxidised hydrocarbons stemming from the oil in the diffusion pump drawing the vacuum on the sample chamber. Since carbon dioxide can be discounted as contributing to the O 1s peak [19], the

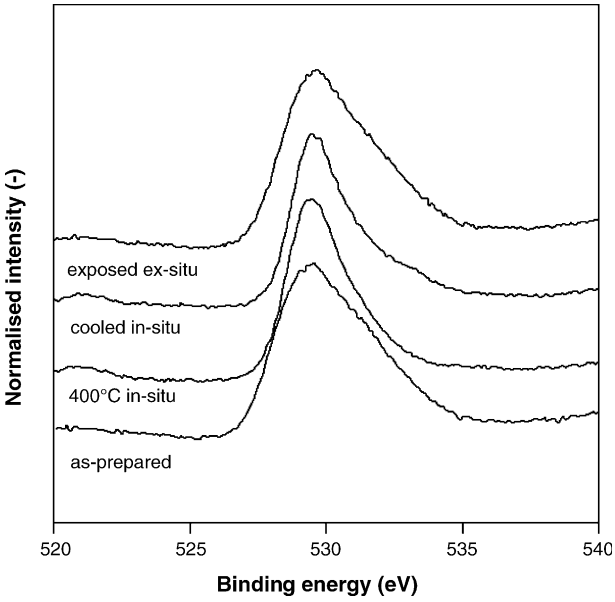

Fig. 1. O 1s XPS spectra for CeO_2-coated $BaTiO_3$ collected in the as-prepared state at RT, at 400 °C, after cooling to RT in the sample chamber, and after cooling to RT while exposed to atmosphere. This series measured for La_2O_3-coated powder exhibits the same trends.

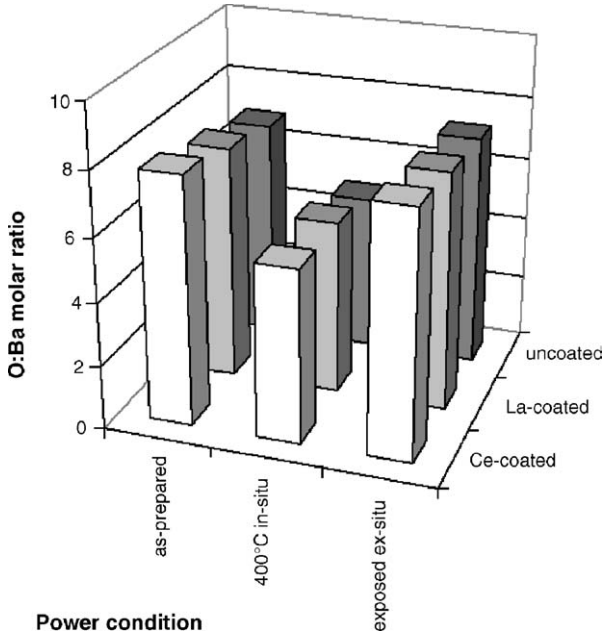

Fig. 2. O:Ba molar ratio of coated and uncoated powders calculated from the O 1s and Ba $3d_{5/2}$ XPS peaks measured in the as-prepared state at RT, at 400 °C, and after cooling to RT while exposed to atmosphere.

observed desorbable high-BE shoulder can only be due to adsorbed molecular water at 533.1 eV [20].

Similar behaviour of the O 1s peak was observed for the La-coated and uncoated $BaTiO_3$ powder.[1] The results are summarized in Fig. 2 in terms of the O:Ba molar ratio (Since the Ba content remained constant for a given powder under all conditions, the O:Ba ratio reflects the change in the area of the O 1s peak due to the desorption/adsorption of oxygen-bearing species, i.e. H_2O.)[2] As can be seen, the method was insufficiently sensitive to detect quantitative differences in adsorbate concentrations between the powders. However, of note is that even at 400 °C under UHV, the measured O:Ba ratios of the coated powders and the uncoated control powder still clearly exceeded the 3:1 ratio expected for $BaTiO_3$. This is probably due to chemisorbed –OH groups, the chemical nature of the adsorbate bond to the surface being confirmed by the need to extensively sputter the samples at 400 °C in order to obtain the 3:1 O:Ba ratio expected for $BaTiO_3$. This indicates, as previously with the as-delivered $BaTiO_3$ powder [19], that the surfaces of the lanthanoid-coated powder particles will in all likelihood be fully hydrated during processing and that dispersants and

[1] In order to provide a realistic comparison with the coated powders, the as-delivered base $BaTiO_3$ powder (analysed in [19]) was subjected to the same aqueous preparation procedures described earlier for coating the powders, but without addition of a dopant nitrate. All subsequent references to the control powder in the text refer to this preconditioned, uncoated powder.

[2] Quantitative analysis calculations were performed with area atomic sensitivity factors of 7.9 and 0.66 for Ba $3d_{5/2}$ and O 1s, respectively [20].

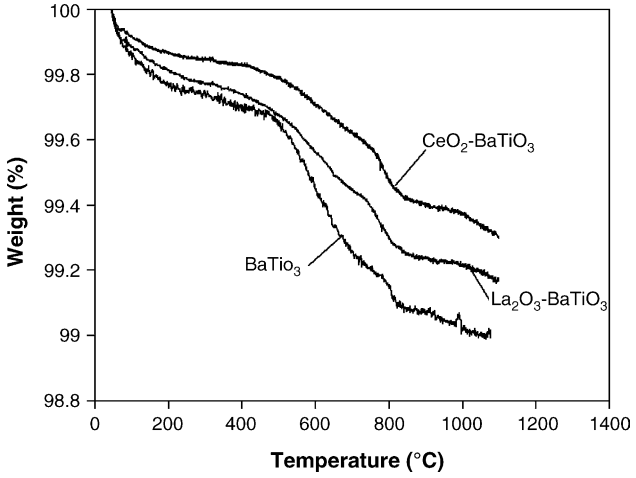

Fig. 3. Weight-loss characteristics of CeO_2- and La_2O_3-coated extrusion powders and uncoated $BaTiO_3$ control powder (5 °C/min, 50 cm^3/min air).

binders will interact with the adsorbed water rather than directly with the ceramic surface.

As shown in Fig. 3, the coated powders experience a small, but distinct, weight loss in several stages up to 1100 °C, as does the control $BaTiO_3$ powder. In conjunction with the conclusions drawn above for the XPS analysis, the initial weight loss around 100 °C is attributed to the loss of physisorbed water. The weight-loss above 400 °C is attributed to the decomposition of $BaCO_3$ which was shown by XRD to be present in all three powders prior to the TGA measurement and absent thereafter (see Fig. 4). This conclusion is in line with published literature regarding $BaCO_3$ decomposition in $BaTiO_3$ systems which also shows the carbonate decomposing in the range 500–900 °C [28,29].

The initial 0.1–0.2 wt.% loss around 100 °C due to physisorbed water agrees closely with the published

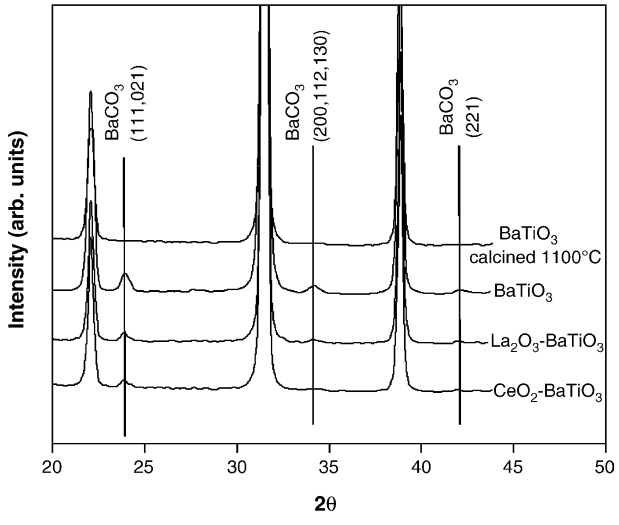

Fig. 4. X-ray diffraction patterns of lanthanoid-coated powders and the uncoated control powder. As with the calcined control powder (shown), the carbonate was removed from the coated powders by calcining at 1100 °C.

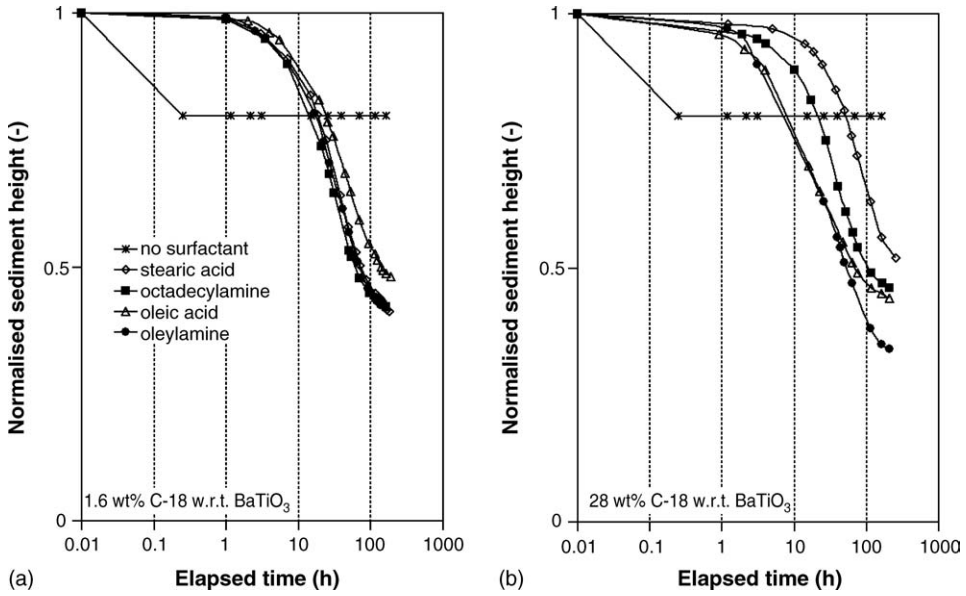

Fig. 5. Sedimentation behaviour of $BaTiO_3$–paraffin mixtures prepared with different C-18 surfactants (80 °C, 10 vol.% solids).

literature [30] and corresponds to a theoretical surface concentration of 5–10 molecules/nm^2. With a single H_2O molecule occupying on order of 0.4 nm^2, this indicates that the powder surfaces are covered by significantly more than a monolayer of water. The data shows that the CeO_2-coated powder has the lowest and the raw $BaTiO_3$ powder the highest moisture content, suggesting that water interacts less strongly with the CeO_2-coated surface than the La_2O_3-coated powder surfaces and that both lanthanoid coatings inhibit water adsorption.

3.2. Surfactant screening

The results of the sedimentation experiments with pure $BaTiO_3$ powder are shown in Fig. 5. Without surfactant, the powder settled to its equilibrium height within 15 min and the sediment consisted of loosely-packed powder spherules 0.2–0.5 mm in diameter. The slower settling rates and higher sediment densities in the presence of the surfactants at both concentrations indicate that they all, to varying extents, disperse and stabilise the powder. However, sharp interfaces between the sediments and their respective supernatants and a complete lack of cloudiness in the supernatants indicated that all the suspensions were to some degree flocculated. The differences in settling rates are attributed to varying degrees of flocculation in the mixtures, with greater flocculation leading to larger secondary particles and faster settling rates [31,32].

Fatty acids with backbones up to 18 carbon atoms long have frequently been associated with the flocculation of ceramic powders in conjunction with organic solvents [6,16,17,21,33–36]. While ≈10 nm separation between micrometre-sized particles is considered a minimum to stabilize a suspension by virtue of steric interactions between opposing adsorbed surfactant layers, C-18 carboxylic acids, for instance, separate neighbouring particles by only ≈4 nm and thus cannot completely overcome the van der Waals forces between particles and prevent entry into the primary attractive potential well between them [34]. Indeed, it has been theorised that such short molecules do not in fact provide any kind of steric potential barrier and only function by keeping the particles further separated and by shielding the van der Waals forces [34]. However, no evidence to support the complete absence of a steric mechanism is given and consequently this is still considered below.

Steric stabilization depends in part on the conformation of the surfactant tails in solution with their solvent and hence on the solubilities of the components with one another. In this situation, Hildebrand–Hansen solubility parameters provide a convenient gauge with which to predict solubilities between liquids, i.e. liquids with similar parameters will generally be soluble in one another while those with dissimilar values will be insoluble [37]. The dispersive solubility parameters (δ_d) describing the cohesive effects stemming from dispersive interactions between the surfactant carbon chains ($\delta_{d,stearic\ acid}$ = 16.4 MPa$^{1/2}$ and $\delta_{d,oleic\ acid}$ = 14.3 MPa$^{1/2}$) closely bracket that of the solvent oil ($\delta_{d,paraffin\ oil}$ = 14.5 MPa$^{1/2}$), and hence their solubilities are expected to be equal and both types of surfactant tail will be well extended into solution. Similar data is not available for the amine surfactants, but the different polar head group is not expected to change the dispersive component of these species. On this basis, solubility differences leading to changes in tail conformations are discounted as causing the observed differences in stabilisation.

At 1.6 wt.% C-18 corresponding to theoretical monolayer coverage of the powder by stearic acid, differences in the

sedimentation behaviour between the surfactants cannot be distinguished except for a slightly better stability imparted by the oleic acid. Considering that the estimated surface area occupied per oleic acid molecule (0.4 nm^2) [6] is twice that of a stearic acid molecule (0.2 nm^2) [22], the 1.6 wt.% oleic acid concentration nominally corresponds to twice monolayer coverage and thus this suspension must have a higher free surfactant concentration than the stearic acid system. While steric repulsion is proportional to the volume fraction of chains in the adsorbed layer [38] and thus any steric effects will be reduced for the oleic acid case, the free oleic acid component appears be functioning as a depletion stabiliser and shows, as postulated previously, that dispersion stability is a function of both the free [35,39,40] and the surface [6,33] concentration of the surfactant. While the same molecular footprint and concentration considerations apply to the two amine surfactants, different concentration equilibria appear to be operating whose combined effects balance out to generate apparently equal stability.

At 28 wt.% C-18, where the surfactant/binder (i.e. paraffin) ratio approximates that found in highly-loaded extrusion pastes, the suspensions with stearic acid and octadecylamine exhibit the best stability. McNulty et al. [39] have postulated that surfactant adsorption to a solid surface increases as the concentration of the surfactant in the solvent (or binder) approaches the solubility limit. Comparing the melting temperatures of the surfactants with saturated carbon bonds ($T_{m,stearic\ acid} = 70\ ^\circ C$, $T_{m,octadecylamine} = 51\ ^\circ C$) to those with a C=C bond in their carbon chain ($T_{m,oleic\ acid} = 6\ ^\circ C$, $T_{m,oleylamine} = 25\ ^\circ C$), the former two surfactants must be significantly closer to their solubility limit at the sedimentation temperature of 80 °C than their unsaturated counterparts. Therefore, the driving force for adsorption will be greater for stearic acid and octadecylamine, and consequently the surface concentration should be higher and the stabilisation effect better, and this is indeed what the sedimentation data shows. The better stabilisation imparted by stearic acid relative to octadecylamine is attributed to the greater dipole moment of the COOH group relative to the $–NH_2$ group leading to better adsorption on the water-saturated (i.e. polar) $BaTiO_3$ powder surface.

Based on these sedimentation results, stearic acid was chosen as the surface active species to be used in the remainder of this work. A sedimentation experiment with stearic acid was performed to evaluate the behaviour of coated powders (CeO_2–$BaTiO_3$; La_2O_3–$BaTiO_3$) in paraffin suspensions. Fig. 6 shows that the settling velocity of both coated powders is significantly faster than for the uncoated powder, and that the Ce-coated powder settles faster than its La-coated counterpart. The slight particle coarsening and agglomeration observed as a consequence of the coating procedure and noted earlier is not expected to have such a marked effect on the settling rate, thus the loss of stability is attributed to the presence of the dopant coatings reducing adsorption of the surfactant. In this light, it appears that the stearic acid adsorbs less effectively on CeO_2-coated powder, causing its suspension in paraffin to be slightly less stable than the La_2O_3-coated powder.

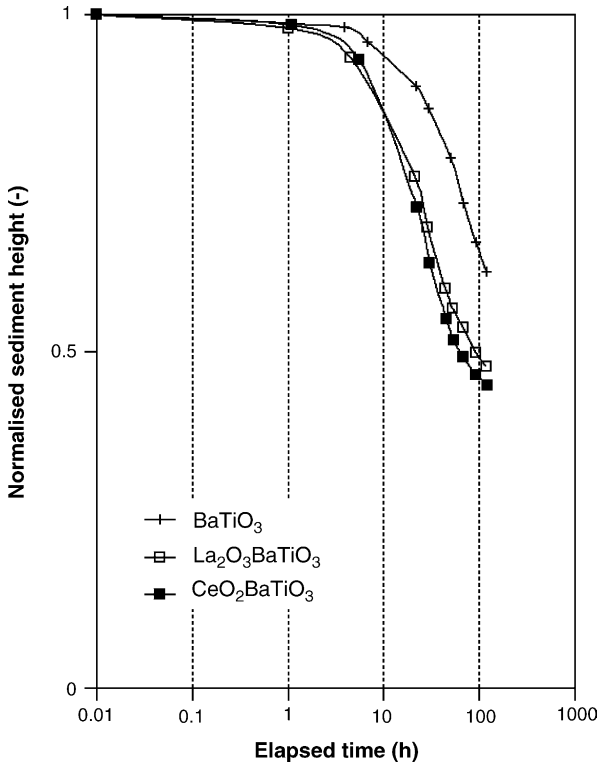

Fig. 6. Sedimentation behaviour of coated and uncoated control powders in paraffin suspensions prepared with stearic acid (80 °C, 10 vol.% solids, 28 wt.% stearic acid w.r.t. $BaTiO_3$).

The parallel trends of water adsorption (XPS analysis) and stearic acid adsorption apparent from the above data provides further evidence that the surfactant interacts with the adsorbed water layers rather than directly with the ceramic surface.

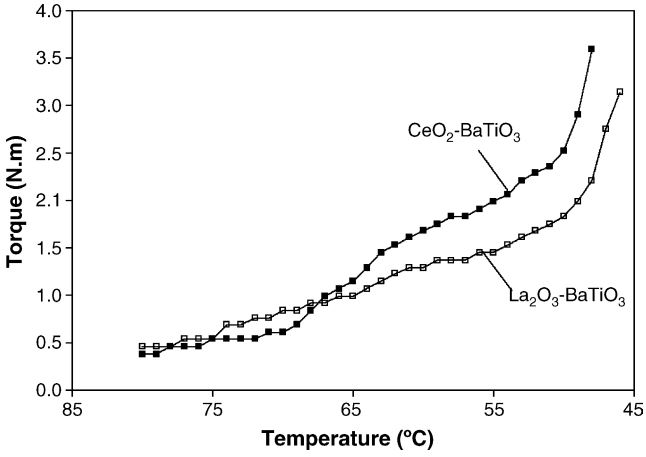

Fig. 7. Mixing-torque evolution upon cooling of feedstocks with coated powders at 50 vol.% solids loading.

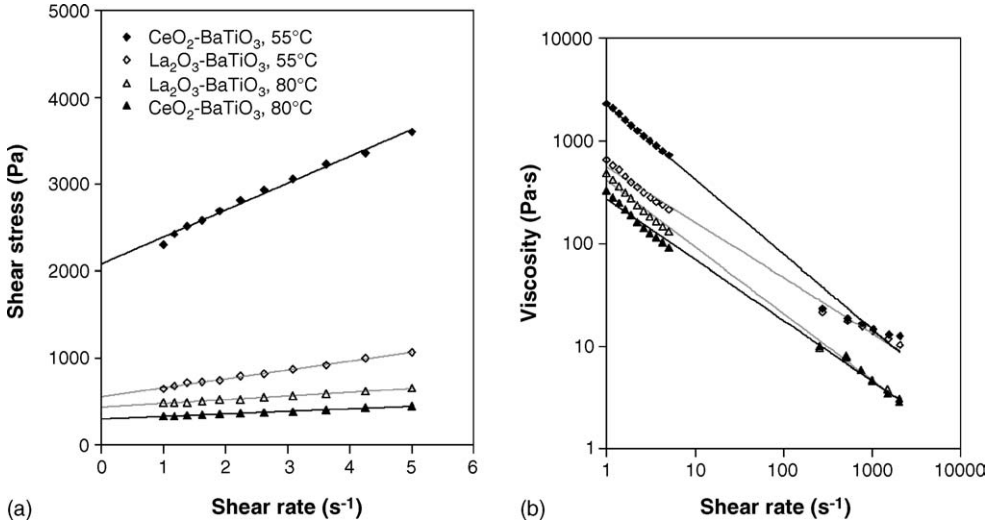

Fig. 8. Rheological behaviour of 50 vol.% feedstocks with coated powders: (a) shear stress as a function of shear rate and (b) viscosity as a function of shear rate.

3.3. Powder-polymer extrusion feedstocks

On the basis of the differences observed in the dispersion state at low solids loading (10 vol.%; Fig. 6) and the adsorbed water concentration between the two lanthanoid-coated powders, differences in the rheological behaviour at higher loadings for use in extrusion (50 vol.%) were not unexpected. The torque-temperature cooling curves in Fig. 7 which were recorded at the conclusion of feedstock mixing reveal that while the viscosity of the La_2O_3-containing paste increases monotonically while cooling from 80 to 55 °C, the viscosity of the CeO_2-doped mix exhibits a marked increase upon cooling through 70 °C so that it ultimately has a higher viscosity than the La_2O_3-doped formulation. This reversal of the relative viscosity magnitude is also apparent in the rheological analysis of the feedstocks, as shown in Fig. 8.

This behaviour may be explained, as above, by less stearic acid being adsorbed on the CeO_2-coated than to the La_2O_3-coated powders. While at 80 °C the separation of the CeO_2-coated particles will be impaired, the larger concentration of surfactant molecules in solution will act to lower the viscosity of the binder [33,41] and possibly contribute to particle separation via the depletion stabilisation mechanism. Upon cooling through the solidification temperature of stearic acid at 70 °C, the free stearic acid molecules will aggregate, thereby effectively removing plasticiser from the binder and increasing its viscosity. Additionally, the depletion stabilisation mechanism, if it is indeed acting, will be less effective, which, together with the lower surfactant surface concentration, results in more interparticle contact than in the La_2O_3–$BaTiO_3$ system and leads to the viscosity trend reversals shown in Figs. 7 and 8. Liu previously noted [17] that the behaviour of a surfactant upon changing the temperature in the vicinity of its melting point may have a profound effect on the rheological properties of a suspension, and the current data clearly confirms this hypothesis.

Fig. 8 also shows that the $BaTiO_3$/paraffin/stearic acid system possesses a yield point and is shear thinning. This behaviour enabled the generally successful extrusion of both feedstocks at 55 °C, i.e. below the solidification temperature of the surfactant. Samples of green extrudates obtained with a 300 μm die are shown in Fig. 9. While La_2O_3–$BaTiO_3$ fibres of 150 and 100 μm diameter could also be extruded at this temperature, this was impossible with the CeO_2–$BaTiO_3$ system. Extrusion at 80 °C proved generally problematical, particularly with the CeO_2-coated system which frequently exhibited binder separation from the powders. In general the extrudability of the CeO_2–$BaTiO_3$ system was inferior to that of its La_2O_3–$BaTiO_3$ counterpart.

As discussed above for the sedimentation data, the lower concentration of adsorbed stearic acid on the CeO_2-coated powder relative to the La_2O_3-coated powder can explain the observed behaviour. The former system would be less well dispersed in the binder and this situation would be exacerbated at 80 °C where thermal activation is likely to promote desorption of surfactant from the powder. This conclusion is supported by the appearance of clear binder droplets at the die exit (i.e. bulk binder separation) during extrusion of the CeO_2–$BaTiO_3$ system at 80 °C which indicates a loss of the chemical bridge between the binder and the powder which the stearic acid is supposed to provide.

Poorer dispersion of the CeO_2-coated powder in the binder should result in wider interparticle pore channels being present in this system than in the La_2O_3–$BaTiO_3$ system, and this is reflected in the pore size distributions of the extrudates. Fig. 10 shows that for interparticle pores on the order of 0.1 μm, the La_2O_3–$BaTiO_3$ samples possesses slightly finer pores than their CeO_2-coated counterparts.[3] The tails toward large pore sizes for the La_2O_3–$BaTiO_3$

[3] While the difference between the distributions is very small, it was reproducible for two pairs of feedstocks prepared separately and for both the debound and presintered states (T_{max} = 750 and 1200 °C, respectively).

feedstocks are due to flattened pores (thickness ≈1–2 μm, axial dimensions ≈5–10 μm) containing pure binder which are visible in the SEM image of the fracture surface of the green La_2O_3–$BaTiO_3$ fibre in Fig. 9b. These flakes, which manifest themselves as ''intraparticle'' pores once the binder is burned out, are also present in the green CeO_2–$BaTiO_3$ fibres, but at a much lower frequency.

The formation mechanism for these pores is unclear. As mentioned in the experimental procedure, extrudable feedstocks with 60 vol.% solids could be prepared with both powders, and neither of the resulting feedstocks exhibited these binder flakes. As such it is clear that there is a connection between the flakes and the ''excess'' binder in the 50 vol.% feedstocks. It appears that it is energetically more favourable for this excess binder to collect into pools rather than to be uniformly distributed between the powder particles, especially in the La_2O_3–$BaTiO_3$ case (For this system it is interesting to note that this localised phase separation occurs without the occurrence of the bulk phase separation observed in the CeO_2–$BaTiO_3$ system.) Shearing motions imposed on the materials during mixing and extrusion cause these pools to form as flattened flakes rather than spherical droplets, a conclusion based on the observation that the in-plane axes of the flakes are always oriented parallel to the fibre axis. The connection between

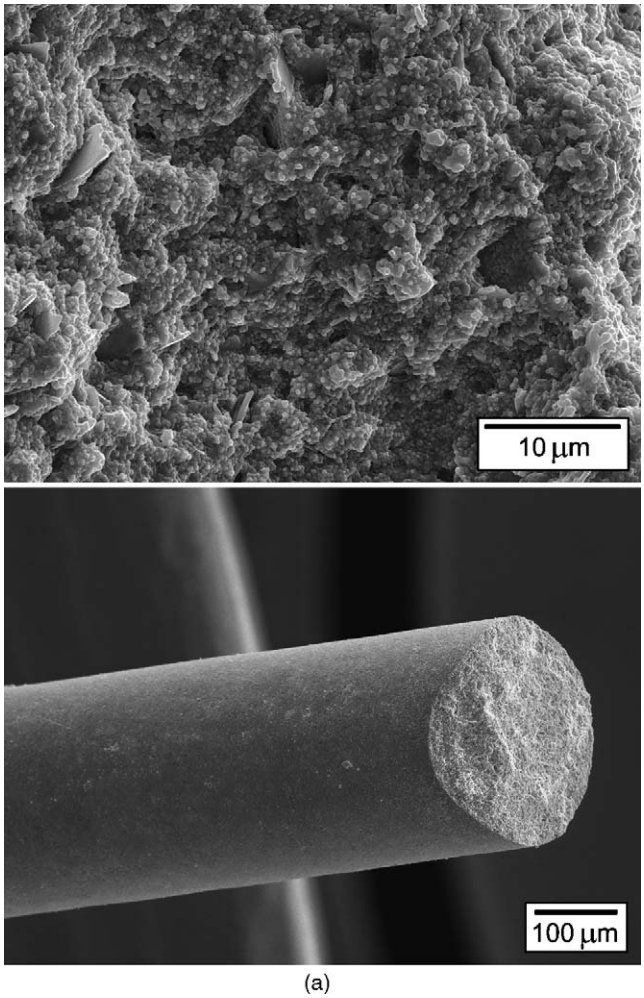

(a)

Fig. 9. SEM image of fibres (top) and their fracture surfaces (bottom) of (a) CeO_2-coated $BaTiO_3$ and (b) La_2O_3-coated $BaTiO_3$ ($T_{extrusion}$ = 55 °C).

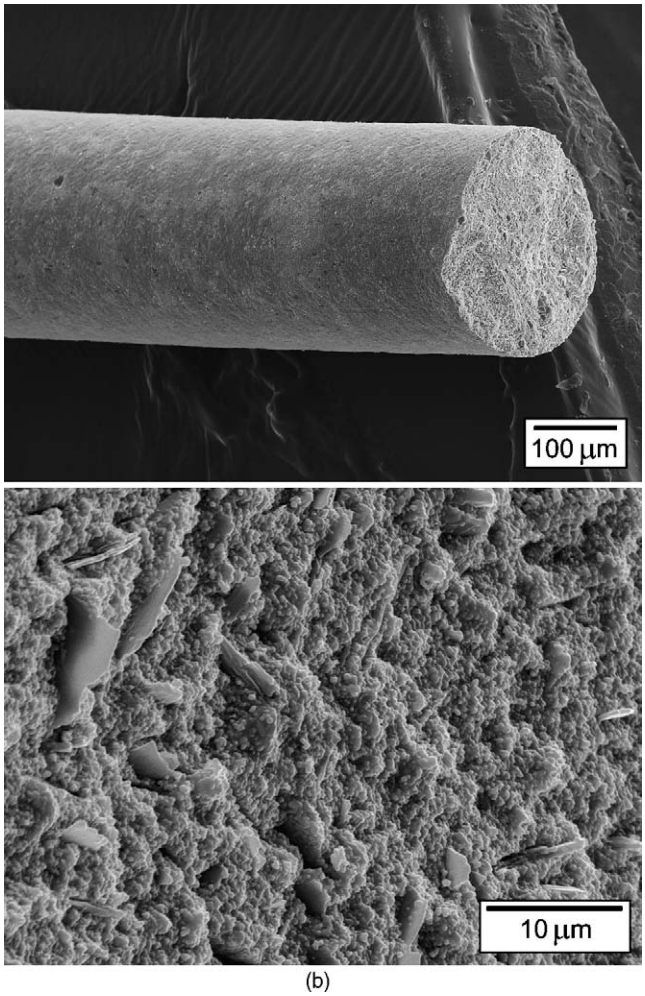

(b)

Fig. 9. (*Continued*).

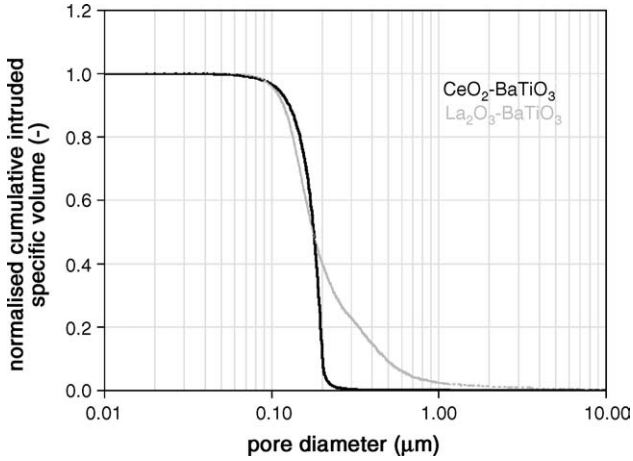

Fig. 10. MIP pore-size distribution of presintered feedstocks (T_{max} = 1200 °C).

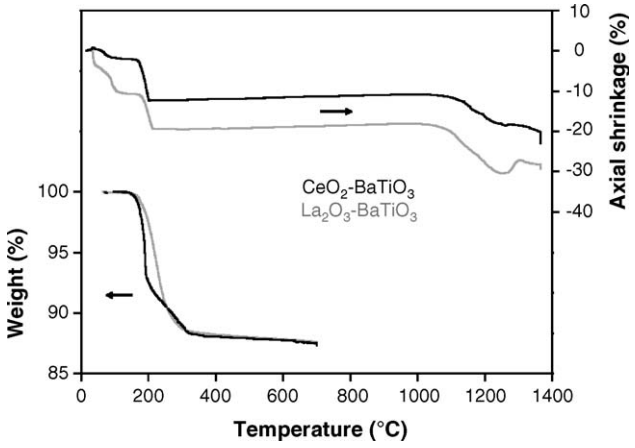

Fig. 11. Weight-loss and shrinkage characteristics during heat treatment of debound 50 vol.% Ce- and La-doped feedstocks (axially-pressed samples, 50 cm^3/min air).

the frequency of the flakes and the powder-paraffin/stearic acid interactions in the two systems remains under investigation.

3.4. Heat treatments

The greater affinity of the stearic acid/paraffin wax binder for the La_2O_3-coated powder than for the CeO_2-coated powder also manifests itself in the TGA and TMA data shown in Fig. 11. The reduced weight-loss rate relative to the Ce-bearing system is indicative of a stronger interaction between the La_2O_3-coated powder and the binder system. Furthermore, the better dispersion state and the collapse of the large intraparticle pores during debinding under the applied pressure of the TMA probe ultimately results in a higher packing density and a greater apparent contraction of the La_2O_3–$BaTiO_3$ sample relative to the CeO_2–$BaTiO_3$ sample. On the basis of this data, the final sintered density of the La-doped composition should be higher than that of the Ce-doped material, and this is indeed the case, with the former reaching 95.8% of theoretical density on average and the latter only 93.6% (determined by image analysis of polished fibre cross-sections). The different shapes of the TMA characteristics above the $BaTiO_3$-AST eutectic temperature at 1240 °C indicate that the dopants also affect the sintering process in these materials, and this effect is still under investigation.

4. Summary

With a view to fabricating fibres of lanthanoid-doped PTCR $BaTiO_3$ by extrusion, a submicron $BaTiO_3$ powder was coated with either cerium oxide or lanthanum oxide. XPS and thermal analysis revealed that the powder particle surfaces are hydrated with layers of physisorbed molecular water and chemisorbed hydroxyl groups and that the CeO_2-coated powder absorbs less H_2O than its La_2O_3-coated counterpart. Screening of four potential 18-carbon carboxylic acid and amine surfactants by sedimentation experiments in molten paraffin wax revealed stearic acid to be the most effectively adsorbed species on $BaTiO_3$ with the greatest stabilising effect. Sedimentation experiments with coated $BaTiO_3$ powders in molten paraffin/stearic acid revealed La_2O_3-coated powder to be better stabilised than CeO_2-coated powder, leading to the conclusion that the surface adsorption concentration of stearic acid is greater in the La_2O_3-doped system.

The coated powders were subsequently mixed with sintering aids and compounded with the paraffin/stearic acid binder at a solids loading of 50 vol.%. The resulting feedstocks exhibited a yield point and shear thinning behaviour, and while both were successfully extruded, the CeO_2–$BaTiO_3$ system exhibited generally inferior extrudability compared to its La_2O_3–$BaTiO_3$ counterpart. This behaviour and the differing microstructures observed at various stages of heat treatment could be attributed to the higher adsorption concentration of stearic acid molecules on the La_2O_3-coated surface.

Acknowledgements

The authors thank all the involved academic and technical staff at Strathclyde University and EMPA for their contributions to this work, and Ferro Electronic Materials for their generous contribution of powder. Special thanks go to Ms. Silvia Hangl for performing the monolayer sedimentation experiments and preparing feedstocks. This work is based in part on the Ph.D. Thesis ‘‘Microextrusion of Barium Titanate for PTCR Applications’’ by M. Wegmann, Department of Mechanical Engineering (Materials and Metallurgy Group), University of Strathclyde, Glasgow, United Kingdom, 2002. Financial support was provided through internal funding resources at EMPA and a Ph.D. research studentship at Strathclyde University.

References

[1] Z.-C. Chen, T. Ring, J. Lemaître, Stabilization and processing of aqueous $BaTiO_3$ suspension with polyacrylic acid, J. Am. Ceram. Soc. 75 (12) (1992) 3201–3208.
[2] Y. Ohara, K. Koumoto, H. Yanagida, Effect of crystal-axis orientation on dielectric properties of ceramics prepared from fibrous barium titanate, J. Am. Ceram. Soc. 77 (9) (1994) 2327–2331.
[3] S. Mizuta, M. Parish, H. Bowen, Dispersion of $BaTiO_3$ powders (Part I), Ceram. Int. 10 (1984) 43–48.
[4] J.-H. Jean, H.-R. Wang, Dispersion of aqueous barium titanate suspensions with ammonium salt of poly(methacrylic acid), J. Am. Ceram. Soc. 81 (6) (1998) 1589–1599.
[5] B. Lee, Chemical variations in barium titanate powders and dispersants, J. Electroceram. 3 (1999) 53–63.
[6] L. Bergström, K. Shinozaki, H. Tomiyama, N. Mizutani, Colloidal processing of very fine $BaTiO_3$ powder—effect of particle interactions

on the suspension properties, consolidation, and sintering behaviour, J. Am. Ceram. Soc. 80 (2) (1997) 291–300.
[7] K. Mikeska, W. Cannon, Dispersants for tape casting pure barium titanate, in: J. Mangels, G. Messing (Eds.), Advances in Ceramics Forming of Ceramics, vol. 9, American Ceramic Society, Westerville, 1984.
[8] T. Chartier, E. Jorge, P. Boch, Dispersion properties of $BaTiO_3$ tape-casting slurries, J. Eur. Ceram. Soc. 11 (1993) 387–393.
[9] U. Paik, Aqueous processing of barium titanate powders, J. Korean Phys. Soc. 32 (1998) S1224–S1226.
[10] M. Blanco-López, B., F. Riley, The isoelectric point of $BaTiO_3$, J. Eur. Ceram. Soc. 20 (2000) 107–118.
[11] M. Wegmann, F. Clemens, T. Graule, A. Hendry, Microextrusion of lanthanide-doped barium titanate for PTCR applications, Am. Ceram. Soc. Bull. 82 (11) (2003) 9501–9508.
[12] B. Huybrechts, K. Ishizaki, M. Takata, Review: the positive temperature coefficient of resistivity in barium titanate, J. Mater. Sci. 30 (1995) 2463–2474.
[13] R. Lenk, A. Krivoshchepov, Effect of surface-active substances on the rheological properties of silicon carbide suspensions in paraffin, J. Am. Ceram. Soc. 82 (2) (2000) 273–276.
[14] H. Suwardie, R. Yazici, D. Kalyon, S. Kovenklioglu, Capillary flow behaviour of microcrystalline wax and silicon carbide suspension, J. Mater. Sci. 33 (1998) 5059–5067.
[15] S. Novak, K. Vidovič, M. Sajko, T. Kosmač, Surface modification of alumina powder for LPIM, J. Eur. Ceram. Soc. 17 (1997) 217–223.
[16] W. Tseng, Influence of surfactant on rheological behaviour of injection-moulded alumina suspensions, Mater. Sci. Eng. A289 (2000) 116–122.
[17] D. Liu, Effects of dispersants on the rheological behaviour of zirconia-wax suspensions, J. Am. Ceram. Soc. 82 (5) (1999) 1162–1168.
[18] Y. Matsuo, M. Fujimura, H. Sasaki, K. Nagase, S. Hayakawa, Semiconducting $BaTiO_3$ with additions of Al_2O_3, SiO_2 and TiO_2, Am. Ceram. Soc. Bull. 47 (3) (1968) 292–297.
[19] M. Wegmann, L. Watson, A. Hendry, XPS analysis of submicron barium titanate powder, J. Am. Ceram. Soc. 87 (3) (2004) 371–377.
[20] D. Briggs, M. Seah, Practical Surface Analysis: vol. 1: Auger and X-ray Photoelectron Spectroscopy, John Wiley & Sons, Chichester, 1996
[21] I. Sushumna, R. Gupta, E. Ruckenstein, Effective dispersants for concentrated, nonaqueous suspensions, J. Mater. Res. 7 (1992) 2884–2893.
[22] W. Moore, Grenzflächen (Interfaces), in: S. Hummel, G. Trafara, K. Holland-Moritz (Eds.), Physikalische Chemie (Physical Chemistry), Walter de Gruyter & Co, Berlin, 1986.
[23] J. Heiber, F. Clemens, T. Graule, Fabrication of SiO_2 glass fibres by thermoplastic extrusion, Glass Sci. Technol. 77 (2004) 211–216.
[24] C. Macosko, Rheology; Principles, Measurements and Applications, VCH Publishers Inc., New York, 1994.
[25] V. Fuenzalida, M. Pilleux, I. Eisele, Adsorbed water on hydrothermal $BaTiO_3$ films: work function measurements, Vacuum 55 (1999) 81–83.
[26] N. le Bars, P. Levitz, A. Messier, M. Francois, H. van Damme, Deagglomeration and dispersion of barium titanate and alumina powders in an organic medium, J. Colloid Interface Sci. 175 (1995) 400–410.
[27] K. Nagata, S. Kodama, H. Kawasaki, S. Deki, M. Mizuhata, Influence of polarity of polymer on inorganic particle dispersion in dielectric/polymer composite systems, J. Appl. Polym. Sci. 56 (1995) 1313–1321.
[28] C. Hérard, A. Faivre, J. Lemaitre, Surface decontamination treatments of undoped $BaTiO_3$—Part I: Powder and green body properties, J. Eur. Ceram. Soc. 15 (1995) 135–143.
[29] M. Delfrate, J. Lemaitre, V. Buscaglia, M. Leoni, P. Nanni, Slip casting of submicron $BaTiO_3$ produced by low-temperature aqueous synthesis, J. Eur. Ceram. Soc. 16 (1996) 975–984.
[30] R. Becker, W. Cannon, Source of water and its effect on tape casting barium titanate, J. Am. Ceram. Soc. 73 (5) (1990) 1312–1317.
[31] C. Allain, M. Cloitre, M. Wafra, Aggregation and sedimentation in colloidal suspensions, Phys. Rev. Lett. 74 (1995) 1478–1481.
[32] W. Tseng, S.-Y. Li, Effect of polysaccharide polymer on sedimentation and rheological behaviour of aqueous $BaTiO_3$ suspensions, J. Mater. Process. Technol. 142 (2003) 408–414.
[33] A. Doroszkowski, R. Lambourne, Effect of molecular architecture of long-chained fatty acids on the dispersion properties of titanium dioxide in non-aqueous liquids, Faraday Discuss. 65 (1978) 252–263.
[34] R. Johnson, W. Morrison, Ceramic powder dispersion in nonaqueous systems, in: G. Messing, K. Mazdiyasni, J. McCauley, R. Harber (Eds.), Advances in Ceramics: vol. 21: Ceramic Powder Science, American Ceramic Society, Westerville, 1987.
[35] V. Moloney, D. Parris, M. Edirisinghe, Rheology of zirconia suspensions in a nonpolar organic medium, J. Am. Ceram. Soc. 78 (12) (1995) 3225–3232.
[36] W. Tseng, K.-H. Teng, The effect of surfactant adsorption on sedimentation behaviours of Al_2O_3–toluene suspensions, Mater. Sci. Eng. A 318 (2001) 102–110.
[37] A. Barton, Handbook of Solubility Parameters and Other Cohesion Parameters, CRC Press, Boca Raton, 1983.
[38] D. Napper, Polymeric Stabilization of Colloidal Dispersions, Academic Press, London, 1983.
[39] T. McNulty, D. Shanefield, S. Danforth, A. Safari, Dispersion of lead zirconate titanate for fused deposition of ceramics, J. Am. Ceram. Soc. 82 (7) (1999) 1757–1760.
[40] A. Ogden, J. Lewis, Effect of nonadsorbed polymer on the stability of weakly flocculated suspensions, Langmuir 12 (1996) 3413–3424.
[41] S. Lin, R. German, Interaction between binder and powder in injection moulding of alumina, J. Mater. Sci. 29 (1994) 5207–5212.